Stress tuning in sputter-deposited MoOx films

Jean-Yvon Faou, Etienne Barthel, Sergey Y. Grachev

Stress tuning in sputter-deposited MoO_x films

J.-Y. Faou[a], E. Barthel[a], S.Y. Grachev[a,1]

[a]*Surface du Verre et Interfaces, UMR 125 CNRS/Saint-Gobain, 39, quai Lucien Lefranc, F-93303 Aubervilliers, Cedex, France.*

Abstract

The evolution of the compressive stress in Mo/MoOx sputter-deposited thin films has been followed in situ during deposition as a function of two parameters: the oxygen flux and the negative voltage bias applied to the substrate. In addition the microstructure of the films has been characterized. Oxygen accumulation at the interface was observed. We describe the origins of the stress in terms of ion bombardment and oxygen incorporation.

Keywords:
Stress, Molybdenum, Molybdenum oxide, MoOx

1. Introduction

Sputter-deposition is widely used in industry as a fast and versatile way of forming film stacks on a substrate. A range of deposition parameters allows for controlling the film microstructure, stoechiometry, internal stress, interfaces and related physical properties such as adhesion, transparency and conductivity, [1]. Generally, sputter-deposition is carried out far from equilibrium conditions as the atoms and ions with high energy (up to several tens of eV) land on a substrate held at low temperatures. This is the main reason for films to exhibit large density of defects and residual stresses.

Intrinsic stresses in a sputter-deposited film are common. These stresses can be desirable or undesirable. On the one hand, large stresses, both tensile and compressive, cause rupture of weak interfaces and cracking and delamination of the stack. For this reason stresses are undesirable in applications. On the other hand films under high stresses can be used for measuring interfacial toughness by means of the superlayer test [2, 3]. The stresses themselves have been a subject of research for decades now for these reasons, in connection with other characteristics of the film such as microstructure.

There are a number of phenomena driving stress evolution while the film is being deposited (see reviews [4, 5, 6]). During the early steps of deposition, island nucleation, growth and coalescence occur which result in an evolution of stress. For thick polycrystalline films (> 100 nm) the resulting residual stress is believed to be mainly defined by the latter processes, mainly grain competitive growth, grain boundary zipping, incorporation of impurities and diffusion and ion peening [7, 8, 9, 10, 11]. For thicker films (> 1 μm) the microstructure and texture develop in complicated way resulting in stress gradients and specific surface morphologies [12, 13]. All these phenomena are sensitive to the deposition and substrate conditions. Often there are several mechanisms competing in stress generation [14]. Consequently, each product requires a fine tuning of deposition parameters for desired mechanical properties. Current knowledge allows for the stress design in film stacks for semiconductor industry and in large area coatings. A general approach is still lacking for more complicated systems such as oxides and other multi-componential films and stacks.

This paper focuses on stress tuning in MoO_x thin films by varying the oxygen partial pressure and bias voltage applied to the substrate during deposition. The stress in the film was monitored *in-situ* during deposition by measuring the curvature of a flexible substrate. We found that the compressive stress in pure Mo film was caused by ion peening while in MoO_x films oxygen incorporation and diffusion contributed to stress generation. We connect microstructural observations with the stress evolution.

2. Experiments

Molybdenum and oxidized molybdenum films are deposited on 2 inch diameter Si(100) wafers with native oxide.

All films are deposited by magnetron sputtering in a high vacuum chamber (base pressure 4×10^{-5} Pa. Deposition pressures range from 0.15 Pa to 0.22 Pa. Sputtering gases are Ar at a fixed flux of 40 sccm and O_2 with varying flux. Films are prepared at room temperature with a DC power of 150 W. Deposition rate ranges from 3.5 – 4 Å.s^{-1}.

The potential of the substrate is controlled during deposition using an external DC power supply and ranges from 0 V to -75 V. In a series of experiments, the potential is left floating. The floating potential is -22.5 V.

Curvature of the sample is monitored in-situ using a multi-beam optical stress sensor built-in-house [15, 16] (MOSS), presented in Fig.1. A laser beam is split by a semi-reflective mirror. The set of parallel beams reflect on the substrate surface with an incoming angle α. The curvature of the sample causes the

[1]Corresponding author. Email address: sergey.grachev@saint-gobain.com

beams to diverge, and the spot positions observed on a screen are linked to the curvature κ at a time t, as

$$\kappa(t) = \frac{cos(\alpha)}{2L}\left(1 - \frac{D(t)}{D_{ref}}\right) \quad (1)$$

where α is the incoming angle with respect to the sample surface, L is the distance between the sample and the screen, D_{ref} is the distance between spots for a flat substrate, and $D(t)$ is the distance between spots at instant t. If we combine (1) with the Stoney formula, the expression of the stress in the film as a function of the initial curvature of the substrate κ_0 and the spot separation becomes

$$\Delta\sigma^{avg}(t) = (\kappa(t) - \kappa_0)\frac{E_s}{6(1-\nu_s)}\frac{t_s^2}{t_f} \quad (2)$$

where E_s, ν_s and t_s are the Young modulus, the Poisson ratio and the thickness of the substrate respectively and t_f is the thickness of the film.

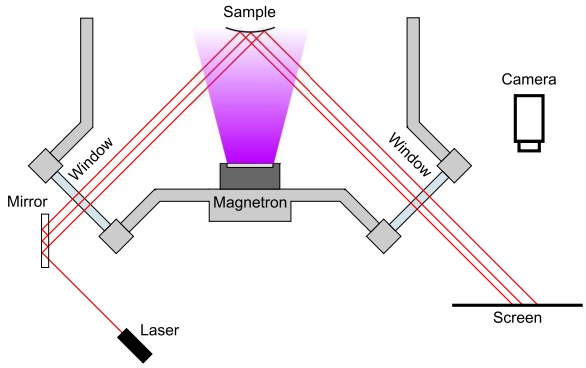

Figure 1: Multibeam optical stress sensor used to measure in-situ the average curvature of the sample during deposition.

Microstructure of the samples is characterized by atomic force microscopy (AFM) for surface roughness. Surfaces are scanned in taping mode with a silicon tip using a Veeco Nanoscope V atomic force microscope. In order to characterize the film cross-sections, we use field emission gun - scanning electron microscopy (FEG-SEM), on a LEO DSM-982 GEMINI microscope operating at 15 kV. We probe oxygen concentration profiles in the films by time of flight secondary ion mass spectrometry (ToF-SIMS). Measurements are perfomed on a TOF-SIMS IV from Ion-Tof and Cs^+ ions are the sputtering species.

3. Results

We begin by studying the influence of the oxygen flux during deposition on the residual stress in the film. In Fig.2 we plot the influence of the oxygen flux on the average stress in the film. The oxygen flux varies from 0 sccm to 4 sccm in the case of the floating potential on the substrate and from 0 sccm to 6 sccm in the case of grounded substrate. (Film thickness is kept at 350 ± 20 nm)

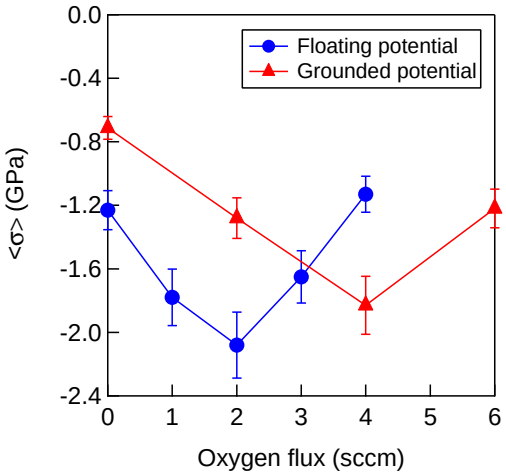

Figure 2: Influence of the oxygen partial pressure on the average stress of the film for two sputtering substrate potential

In case of the floating potential, in the absence of oxygen, we see that the average stress in the film is compressive, around 1.2 GPa. As we increased the oxygen flux, the stress initially becomes more compressive. We observe a maximum in compression around 2.1 GPa in the film when deposited at the oxygen flux of 2 sccm. For larger fluxes, the stress becomes less compressive.

As the potential of the substrate is switched to the ground, we observe similar behavior for the residual stress. The maximum in compression shifts to 4 sccm of O_2 resulting in stress of around 1.8 GPa. Note that the maximum in the average compressive stress is higher in the case of the floating potential than when the substrate is grounded.

Using the MOSS set-up described previously, we then study the stress development in the molybdenum films. In Fig.3 we plot the average stress × thickness versus time for several conditions, which is equivalent to a force per unit of thickness. The slope of the curve provides the value of the local stress in thin film. If the slope is negative the stress is compressive and if the slope is positive the stress is tensile.

In Fig.3a, we observe that the stress is always compressive. As the film thickness increases, the value of compressive stress decreases. When a potential of $-75V$ is applied to the substrate, the stress becomes more compressive with higher compression for small thickness.

In Fig.3b, oxygen is added during the deposition. At floating potential, the stress is also compressive. However the compressive stress is lower for small film thickness. When we apply a potential of -75 V to the sample during growth, we observe the same trend with an overall average compressive stress higher than in the floating potential case.

FEG-SEM images of these four samples are shown in Fig.4. We can see that all the samples exhibit columnar grain structure. The structure remains columnar when a potential of -75 V is applied. However, the addition of oxygen in the MoO_x leads to a reduction of the grain size and at the interface with

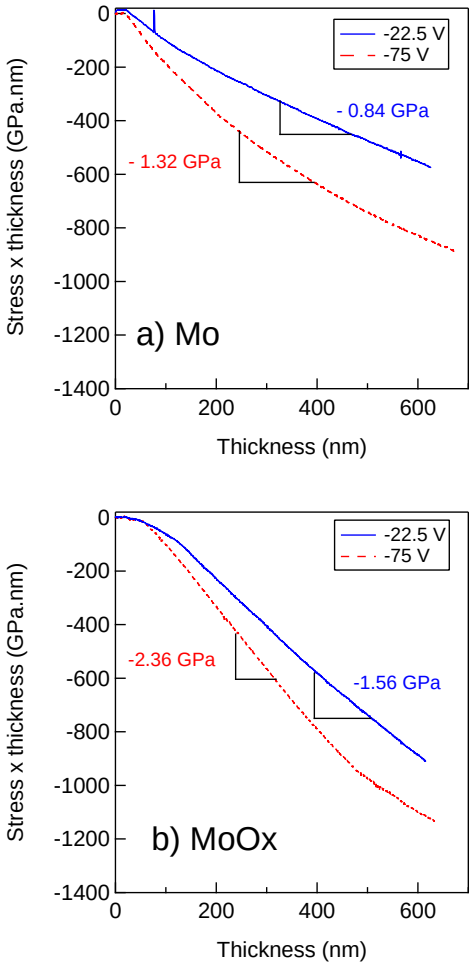

Figure 3: Influence of the substrate potential on stress in molybdenum thin film for (a) no oxygen and (b) 2 sccm of oxygen.

the substrate, the columnar structure of the film has not developed. This layer close to the interface appears amorphous or nanocrystalline.

Root mean square roughness and film thickness, measured by AFM, of four characteristic films are presented in Table.1. We observe that the deposition rate varies by about 10% depending on the deposition conditions. The roughness of the pure molybdenum samples increases when the substrate potential is decreased. For MoO_x films, the roughness is higher when the potential is left floating (−22.5 V).

Sample	Mo		MoO_x	
Potential (V)	-22.5	-75.0	-22.5	-75.0
Thickness (nm)	626.1	671.0	633.0	615.6
Roughness (nm)	6.3	10.8	9.9	4.3

Table 1: Thickness and roughness of five characteristic samples. Deposition times are equal.

Local stress, which is the stress due to a thin layer of thickness dz at a given material thickness z, can be derived from the stress × thickness curves obtained in-situ during the growth of

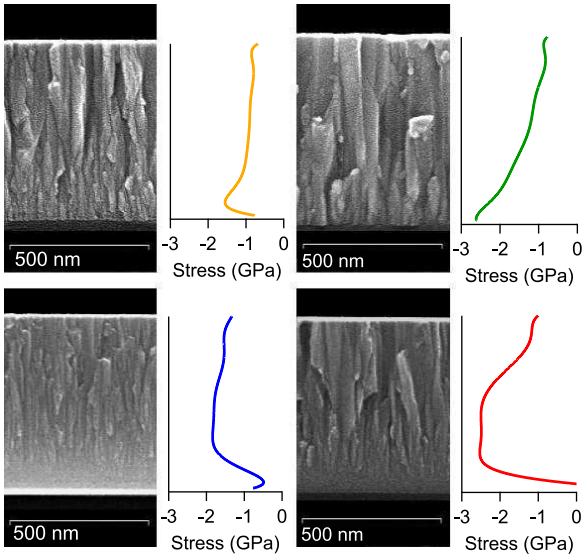

Figure 4: FEG-SEM images showing the influence of substrate potential and oxygen doping on the microstructure of molybdenum thin films. Local stress versus thickness is plotted for each sample. Top left Mo at floating potential, top right Mo at -75 V, bottom left Mo with 2 sccm of O_2 at floating potential and bottom right *Mo* with 2 sccm of O_2 at -75 V.

the film, shown in Fig.3. The measured average stress is related to the local stress by

$$\sigma^{avg} = \frac{1}{h}\int_0^h \sigma^{local}(z)\,dz \tag{3}$$

where $\sigma^{avg}(h)$ is the average stress at a given thickness h and σ^{local} is the local stress. By successively measuring the average stress, via (1), it is possible to evaluate the local stress. We discretize (3) and obtain an iterative formula for the local stress :

$$\sigma_{i+1}^{local} = \frac{1}{h_{i+1}}\left(\sum_1^{i+1} h_k\right)\sigma_{i+1}^{avg} - \frac{1}{h_{i+1}}\sum_1^{i} h_k\sigma_k^{local} \tag{4}$$

Eq.4 should be applied to experimental data with caution. We assume here that the change in curvature observed during the film deposition is only due to new material added, neglecting bulk stress relaxation during deposition.

Mo films deposited without oxygen have high compressive local stress close to the interface as well as medium size grains. In MoO_x films, grains are small at the interface and the stress observed is less compressive than for Mo films. If we look at the local stress behavior and compare it to the microstructure, there is a strong correlation with the grain size.

The XRD patterns of the same samples are shown in Fig.5. All samples exhibit the (110) peak showing that the films are grown as a molybdenum bcc crystalline solid. The presence of stoichiometric oxides, such as MoO_3 phase, are not detected, indicating that the oxygen in the molybdenum films is in interstitial position. However significant differences are observed for films grown with and without oxygen.

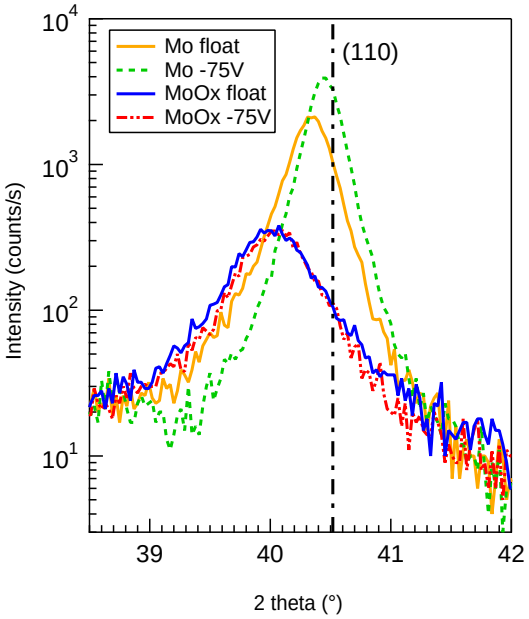

Figure 5: XRD spectra of the same four samples as Fig.4. Dashed line represents the location of the (110)peak of molybdenum.

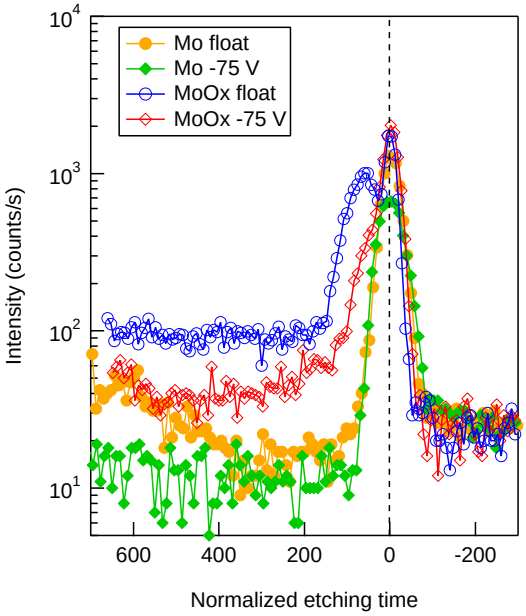

Figure 6: ToF-SIMS measurement of oxygen concentration of the same four samples as Fig.4. Dashed line represents the SiO_2 peak of the substrate interface. MoO_x films have high oxygen concentration at the interface.

The full width at half maximum (FWHM) can be calculated from the spectra presented in Fig.5. The smallest FWHM is obtained for pure Mo at -75 V with 0.28° whereas the value for pure Mo at floating potential is slightly higher 0.32°. The peaks are broader for MoO_x films with a FWHM of 0.66° and 0.63° for Mo with 2 sccm of O_2 at floating potential and Mo with 2 sccm of O_2 at -75 V respectively. The broadening of x-ray diffraction peaks can usually be attributed to the small grain size or the defects in the thin film [17]. When a negative potential is applied during growth of pure Mo, grain size is larger which results in a narrowing of the diffraction peak. This effect is also observed when films are grown with oxygen. From the grain structure of the Mo grown with oxygen presented in Fig.4, we know that the columnar grain size does not differ much between pure and oxydized film. However the large broadening of the peaks is likely to indicate a greater concentration of defects in the films, such as oxygen interstitials.

ToF-SIMS is performed on the same four samples. Concentrations of oxygen through the thickness of the films are presented in Fig.6. We observe that all four samples have a peak of oxygen concentration due to the native oxide of the silicon substrates. Results are normalized to the position of this peak, as the interface reference.

Inside the molybdenum thin film, to the left of the peak of SiO_2, we can distinguish the samples deposited with oxygen as they have between 3 and 10 times higher oxygen concentration through the film than the films deposited without oxygen. The concentration in oxygen is also higher for the films sputtered with floating potential than with the fixed potential of -75 V. This can be explained by the fact that negative oxygen ions are repelled by the applied potential during deposition.

We can also observe a high concentration of oxygen, ten times higher than in the rest of the sample, next to the interface with the substrate in both MoO_x films. The oxygen concentration in the film remains high up to a certain thickness. When we compare the concentration profile of oxygen with the cross-section of the MoO_x films in Fig.4, the oxygen-rich layer corresponds to the nanocrystalline layer and the lower concentration corresponds to the columnar structure.

4. Discussion

Our results suggest that the oxygen content and the microstructure drive the local stress generation. These phenomena can be discussed in relation to the deposition conditions.

The mean free path of atoms with the deposition pressure used (~ 0.22 Pa) is of the order of 10 centimeters or more while the distance between the target and the sample is set to ~ 11 cm. In such conditions the atoms and positive ions [18, 19] reach the sample surface with a wide range of energies reaching up to 10 eV. The oxygen negative ions are accelerated in the electric field and this acceleration leads to a distribution in energy up to 300 eV [20]. Such energies are characteristic of the so-called "ballistic" regime at low processing pressures. The high energy species normally cause the formation of dense films which are often under compression (atomic or ion peening effect [21]).

All these effects seem to play a role in the formation of our Mo MoO_x films. The increase of the average compressive stress in the film with the increase of the negative potential is attributed to the more energetic positive ions bombardment (Ar^+, Mo^+). When the potential is switched to the ground, the bombardment from positive species is reduced and less compression

is developed. Such behavior has been reported previously for chromium thin films [22].

In the case where a columnar microstructure is observed, the presence of oxygen in the plasma also adds to the compression in the film. This is due to incorporation of O atoms in interstitial sites of Mo lattice. Such mechanism by O contamination of pure Mo films has been reported [11]. Remarkably, increase of the negative potential results in higher compression, but lower oxygen content in the film. This can be due to the fact that O^- ions with energies below 75 eV are being repelled by the negative potential on the sample and do not reach the surface. The bombardment by the positive ions, however, is increased like in the case of oxygen-free deposition, which results in still higher compression in the film.

The formation of an amorphous or nanocrystalline interface layer with relatively small stress when oxygen is added to the plasma is not easily explained. One of the plausible explanations is that oxygen directly inhibits the Mo adatoms mobility. This results in the formation of smaller grains with higher density of grain-boundaries. Since the grain-boundaries often cause the tensile stretching of the grains, this effect might have negated the compressive stress due to ion-peening. The high grain boundary density in the nanocrystalline layer and the order of magnitude difference in oxygen concentration between this layer and the columnar structure indicates different sticking coefficient of oxygen during deposition and that most of the oxygen is likely to lie within the grain boundaries.

Stress behavior under increasing oxygen flux can be interpreted considering the change in microstructure from columnar to amorphous. For small amount of oxygen, the film structure remains columnar and O^- bombardment results in the increase of compression observed for both potentials. For a higher flux of oxygen, a less compressive nanocrystalline layer close to the interface is formed. The average compression in the film is therefore reduced.

As the films get thicker, the average stress generally decreases. Partly, this could be due to the heating of the sample by ion bombardment and subsequent relaxation of defects. Enlargement of the grains with thickness may also play a role. One of the consequences of the grain growth is the appearance of voids at the grain-boundaries, which could cause relaxation of the compressive stress.

5. Conclusions

We have observed the stress evolution in Mo/MoO_x films by in-situ curvature measurement. This study was coupled with microstructural characterization by SEM, XRD and ToF-SIMS. In general, the films exhibited a columnar microstructure. The admixture of oxygen resulted in drastic increase of the compression in the film due to oxygen incorporation and enhanced ion bombardment. However, when more oxygen was added (> 2 sccm), the stress seemed to saturate and then decreased. In the MoO_x films, we found an increased oxygen concentration at the interface, which indicated oxygen penetration into the layer upon landing and/or oxygen diffusion. This correlates with the electron microscopy observations, where the interface seemed to be amorphous or consisting of small grains. Negative bias at the substrate resulted in increase of the compression both with and without oxygen. This must be due to higher energy and flux of positive ions bombarding the sample.

6. Acknowledgments

The authors wish to thank Dr. J.E. Greene for interesting discussions. This work was supported by the ANR project number MatetPro07_247145 "Merethif".

References

[1] D.L. Smith, Thin film deposition. McGraw-Hill, Inc. (1995).
[2] A. Lee, B.M. Clemens, W.D. Nix, Acta Mater. 52 (2004) 2081.
[3] S.Yu. Grachev, A. Mehlich, J.-D. Kamminga, E. Barthel, E. Sndergård, Thin Solid Films 518 (2010) 6052.
[4] R. Aberman and R. Koch, Thin Solid Films 142 (1986) 65.
[5] W.D. Nix, Met. Trans. A 20 (1989) 2217.
[6] R.P. Vinci, J.J. Vlassak Annu. Rev. Mater. Sci. 26 (1996) 431.
[7] J.A. Thornton, D.W. Hoffman, Thin Solid Films 171 (1) (1986) 5.
[8] F. Spaepen, Acta Mater. 48 (2000) 31.
[9] E. Chason, D.W. Sheldon, L.B. Freund, J.A. Floro, S.J. Hearne, Phys. Rev. Lett. 88 (2002) 156103.
[10] G.C.A.M. Janssen, A.J. Dammers, V.G.M. Sivel, W.R. Wang, Appl. Phys. Lett. 83 (2003).
[11] L.P. Kendig, Z.U. Rek, S.M. Yalisove, J.C. Bilello, Surf. Coat. Technol. 132 (2000) 124.
[12] S.Y. Grachev, F.D. Tichelaar, G.C.A.M. Janssen, J. Appl. Phys. 97 (2005) 073508.
[13] A.J. Detor, A.M. Hodge, E. Chason, Y.Wang, H.Xu, M.Conyers, A.Nikroo, A.Hamza, Acta Mater. 57 (2009) 2055.
[14] A.A. Navid, E. Chason, A.M. Hodge, Surf. Coat. Technol. 205 (2010) 2355.
[15] J.A. Floro, S.J. Hearne, J.A. Hunter,P. Kotula, E. Chason, S.C. Seeel, C.V. Thompson Journal of Applied Physics 89.9 (2001) 4886.
[16] A. Fillon, G. Abadias, A. Michel, C. Jaouen Thin Solid Films 519 (2010) 1655.
[17] B.E. Warren, X-Ray Diffraction, Addison-Wesley Publishing Co. (1969).
[18] D. Herrmann, M. Oertel, R. Menner, M. Powalla Surface and Coatings Technology 174 175 (2003) 229.
[19] N. Martin, A.M.E. Santo, R. Sanjines, F. Levy Surface and Coatings Technology 138 (2001) 77.
[20] Petr Pokorny, Jiri Bulir, Jan Lancok, Jindrich Musil, Michal Novotny Plasma Process. Polym. 7 (2010) 910.
[21] F.M. dHeurle, Metallurgical Transactions 1 (1970) 725.
[22] G.C.A.M. Janssen, J-D. Kamminga Appl. Phys. Lett. 85 (2004).